Monitoring Stratospheric OClO with Sentinel-5p (S5pOClO)

Sentinel-5p + Innovation - Theme 2: Chlorine Dioxide

Validation Report

document number	:	S5p+I_OCLO_BIRA_VR
authors	:	Gaia Pinardi, Andreas Richter, Andreas Meier, Michel Van Roozendael
Distributed to	:	Christian Retscher
issue	:	1.1
date	:	2020-12-07
status	:	final
Data contributors	:	Myojeong Gu, Thomas Wagner, Kristof Bognar, Ramina Alwarda, Kimberly Strong, Udo Friess, Richard Querel, Cristina Prados-Roman, Margarita Yela Gonzalez

Contents

1 Purpose and objective

The purpose of this Validation Report (VR) is to describe the validation performed on the S5P+I Level-2 OClO product. It contains a review of collected OClO ground-based datasets, the OClO SCD comparison methods, and a summary of ongoing validation results.

This document will be maintained during the development phase and the lifetime of the data products. Updates and new versions will be issued in case of changes in the processing chains or for novel validation exercises.

2 Document overview

Section 4 gives a summary of the requirements on OClO retrievals, Section 5 presents shortly the S5p OClO dataset v0.9 validated here and Section 6 introduces the ground-based data used for this validation report. Section 7 contains a description of the validation approach and Section 8 presents the results, as a function of different estimators.

3 References, terms and acronyms

3.1 References

[AD1] Sentinel-5p Innovation (S5p+I) - Statement of Work - EOP-SD-SOW-2018-049, Issue 2, 20/08/2018.

[AD2] Copernicus Sentinels 4 And 5 Mission Requirements Traceability Document, EOP-SM/2413/BV-bv, Issue 2.0, 7 July 2017.

[AD3] Sentinel-5 Level-2 Prototype Processor Development Requirements Specification, ESA, S5-RS-ESA-GR-0131, issue 1.7, 2018-06-29.

[AD4] Monitoring Stratospheric OClO with Sentinel-5p (S5pOClO), ATBD, S5p+I_OCLO_IUP-UB_ATBD, issue 0.2.1, 9 November 2020.

3.2 Terms, definitions and abbreviated terms

ATBD	Algorithm Theoretical Base Document
AC SAF	Atmospheric Composition Monitoring Satellite Application Facility
CTM	Chemistry Transport Model
DOAS	Differential Optical Absorption Spectroscopy
ESA	European Space Agency
GB	Ground-based

IASB-BIRA	Belgian Institute for Space Aeronomy
IUP-UB	Institute of Environmental Physics (Institut für Umweltphysik), University of Bremen
OMI	Ozone Monitoring Instrument
RTM	Radiative Transfer Model
SZA	Solar Zenith Angle
S-4, -5, -5P	Sentinel-4, -5, -5-Precursor
TROPOMI	TROPOspheric Monitoring Instrument
VR	Validation Report

4 Product requirements

S5p OClO scientific product requirements are mostly determined by the need to monitor stratospheric chlorine activation over time in order to document the continuing effectiveness of the measures taken in the Montreal Protocol and its amendments. Recent reports of unexpected emissions of CFCs (Rigby et al., 2019) underline the relevance of such monitoring. While OClO observations do not provide a direct measure of stratospheric chlorine concentrations, they are an indicator of stratospheric chlorine activation.

For long-term stratospheric monitoring, the most important aspect of the OClO data set is its internal consistency in order to draw reliable conclusions on atmospheric changes. For scientific applications outside of polar stratospheric ozone research such as detection of OClO in lee waves or volcanic emissions, the scientific requirements are mainly the avoidance of false positive detection in the presence of aerosols, clouds and temperature changes and a low noise.

To the knowledge of the authors, no operational thresholds or relative uncertainty requirements have been defined for OClO slant columns for any S5p/S5/S4 instrument so far. For the AC SAF OClO GOME2 product, there were general requirements: Threshold accuracy: 100%; Target accuracy: 50%; Optimal accuracy: 30%. Typical OClO slant columns observed at 90° SZA in the fully activated vortex are of the order of 2×10^{14} molec/cm^2. For GOME2, standard deviations of 6×10^{13} molec/cm^2 are found for individual measurements and systematic differences between the different GOME instruments of the order of 1-2x 10^{13} molec/cm^2 (Richter et al., 2015).

The requirements for ground-based datasets are related to their polar location, for the OClO sampling, and their quality. Quality assurance of the ground-based datasets involves the reporting of the error and a common verification for possible offsets (see Sect. 6.1.1).

5 S5p OClO data

The current document focuses on the validation of TROPOMI OClO v0.9, that is briefly summarized in the following Table 5.1. Two years of data have been analysed and provided for the validation. An illustration of the OClO values over the 4/2018 to 4/2020 period is given in Figure 5.1.

Table 5.1: Description of the TROPOMI OClO datasets used in this study.

Analysis details	TROPOMI OClO v0.9	
Analysis window	345-389nm	
Cross-sections		
OClO	213 K	Kromminga et al., 1999
NO_2	220 K	Vandaele et at., 2002
O_4	293K	Thalman & Volkamer, 2013
O_3	223 K	Serdyuchenko et al., 2014
	243 K	Serdyuchenko et al., 2014
Ring		Vountas et al., 1998
Mean fit residual northern hemisphere		Derived from single orbit orbit: 906220810 latitude: 60° -- 90° longitude: -180° -- 180°

Mean fit residual tropical pacific		Derived from single orbit, orbit: 902012216 latitude: -10° -- -30° longitude: 200° -- 270°
Polynomial	5. Order (6 coeffs.)	
Background spectrum	Daily irradiance	
Post-processing	Destriping, no offset correction	

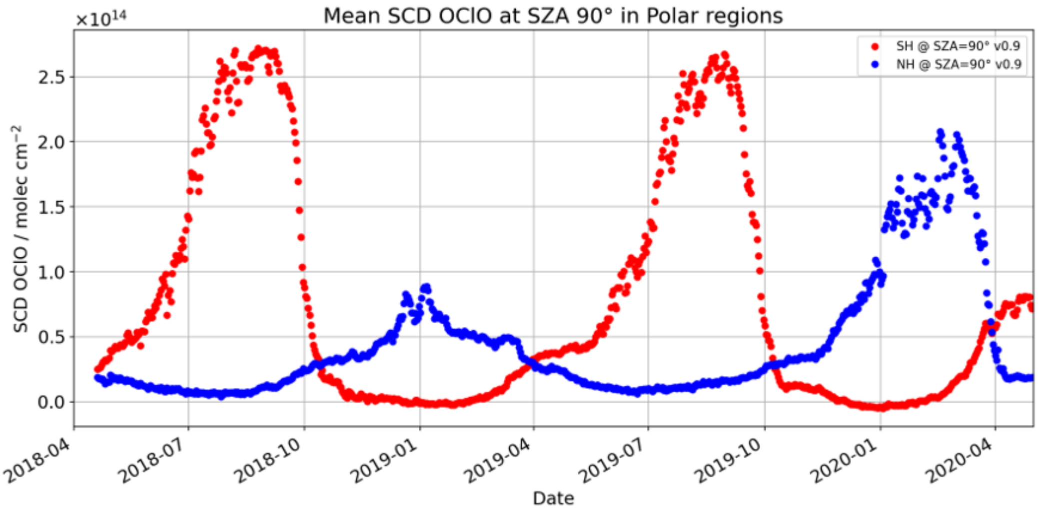

Figure 5.1: Time-series of daily TROPOMI mean OClO SCD around 90° SZA over Polar regions, separated by Southern Hemisphere (red) and Northern Hemisphere (blue).

The two-year time series starts in April 2018 with the continuous availability of S5p spectra. The time span until May 2020 covers the activation period twice in both hemispheres. A similar magnitude and duration of the activation period is observed for both southern hemispheric winters, as it is expected due to the usually stable southern polar vortex. For the northern hemisphere, the polar vortex is not as stable and chlorine dioxide levels which depend on the degree of chlorine activation on PSCs forming in the cold vortex area are more variable.

For the current version of the S5p Prototype Product, a precision (1σ) of about 2.5×10^{13} molec/cm^2 is estimated from the scatter in the equatorial Pacific.

6 Reference measurements

In this version of the VR, only comparisons with ground-based data are included. Comparisons with other satellite datasets and some model results will be included in a next version of this document.

6.1 Ground based monitoring network

OClO columns have been retrieved from the ground since 1986 using Differential Optical Absorption Spectroscopy (DOAS) measurements in the Antarctic and Arctic (Solomon et al., 1987; 1988; Kreher et al., 1996; Gil et al., 1996; Richter et al., 1999; Tørnkvist et al., 2002; Vandaele et al., 2005; Friess et al., 2005).

Several zenith-sky DOAS instruments operating in the NDACC (https://www.ndaccdemo.org/) framework produce OClO slant columns, albeit usually not as their primary product. These data sets are available from the instrument operators. For this study, stations situated above 60° latitude (north and south) have been selected and OClO SCD data retrieved from different groups have been collected and used for validation of S5p OClO columns. An overview on the data available is given below and in Table 6.1.

Arctic:

- UToronto operates the PEARL UV-VIS spectrometer in Eureka (Nunavut, northern Canada). OClO SCD data have been analysed with a daily reference since 2007, and with a fixed annual reference since 2018.
- IUP-Bremen operates a UV-VIS spectrometer in Ny-Ålesund (Spitsbergen) since 1995 (Wittrock et al., 2004). OClO SCDs have been analysed since 2007 using one fixed reference for each season.
- MPIC operates a UV-VIS spectrometer in Kiruna (Sweden) since 1996. OClO SCDs have been analysed for since 2007, with a special focus on the 2018-2020 period for the TROPOMI validation.
- BIRA-IASB operates a UV-VIS spectrometer in Harestua (Norway) since the ’90. End of 2012 a new instrument has been installed with an improved signal to noise ratio, and OClO SCDs have been analysed since then using daily annual reference spectra.

Antarctic:

- IUP-Heidelberg operates a UV-VIS spectrometer in the German research station of Neumayer (the ice shelf in the Atlantic sector of the Antarctic continent) since the ’90 (Friess et al., 2005). Generally enhanced OClO signals are observed between August and October, when the polar vortex is over the station.
- IUP-Heidelberg operates a UV-VIS spectrometer in Arrival Heights (78°S, 167°E), part of the New Zealand station Scott Base on Ross Island since the ‘90 (Friess et al., 2005). Another instrument was present at the station, operated by NIWA (Kreher et al., 1996), but stopped measurements in 2017.
- INTA operates a UV-VIS spectrometer in the Belgrano II station, the Argentinian station situated on the coast of the Antarctic continent in the Weddell Sea area. Belgrano is representative of an in-polar vortex station during winter-spring season until the vortex breakdown (Yela et al., 2005, Puentedura et al. 2014). The UV instrument is measuring since February 2011 and OClO SCD have been analysed by INTA for 2011, 2015, 2016, 2018 and 2019. Ground-based SCDs are made outside of the polar night period (mid-April to end of August).
- INTA operates a UV-VIS spectrometer at the Argentinian Marambio station, in Marambio Island (Graham Land, Antarctic Peninsula) since 2015. Marambio is frequently located in the vortex edge region and affected by both vortex air masses and mid-latitude air masses.

It can be seen in Figure 6.1 that this dataset ensures a good temporal coverage, with the different stations measuring at least one year in overlap with the S5p dataset (April 2018 to March 2020). A good coverage of the Arctic and Antarctic regions is also assured, with half of the stations in the Northern Hemisphere and half in the Southern Hemisphere. However, as briefly described in Table 6.2, the ensemble of ground-based datasets is an aggregate of existing measurements and there is no harmonization in the retrieval choices of the different groups processing the OClO data. Different wavelength regions for the OClO analysis have been used by each group, depending on their instrument's wavelength coverage and their sensitivity. The statistical error in OClO SCDs during twilight is on the order of 2 x10^{13} molec/cm² (Friess et al., 2005) for Neumayer and Arrival Heights. Sensitivity tests are ongoing to better characterize the impact of the different DOAS retrieval choices (OClO cross-sections, wavelength ranges, interfering species, the Ring effect, …) and to better assess the ground-based dataset consistency. Systematic uncertainties related to the OClO cross-section (Kromminga at al., 2003 at 213K with respect to other temperatures or with respect to Wahner et al., 1987 choice) are e.g., on the order of 6% to -12% when tested on a few days of Ny-Ålesund OClO SCD analysis. Random SCD errors are estimated by each group in their DOAS analysis, and values for the different datasets range from 6 to 18% for an SCD of about 1.5 x10^{14} molec/cm².

Table 6.1: Overview on ground-based data sets available

Location	Coordinates	Data Provider	Time Coverage
Eureka	80.05°N, 86.42°W	UToronto	2006-present
Ny-Ålesund	78.9°N, 11.9°E	IUPB	1995-present
Kiruna	67.9°N, 20.4°E	MPIC	1997-present
Harestua	60.22°N, 10.75°E	BIRA-IASB	1998-2013 2012-present
Marambio	64.3°S, 56.7°W	INTA	2015-present
Neumayer	70.62°S, 8.27°W	IUPH	2006-present
Arrival Heights	77.83°S, 166.65°W	IUPH NIWA	2006-present 2007-2017 (NIWA)
Belgrano	77.9°S, 34.6 °W	INTA	2011; 2015-present

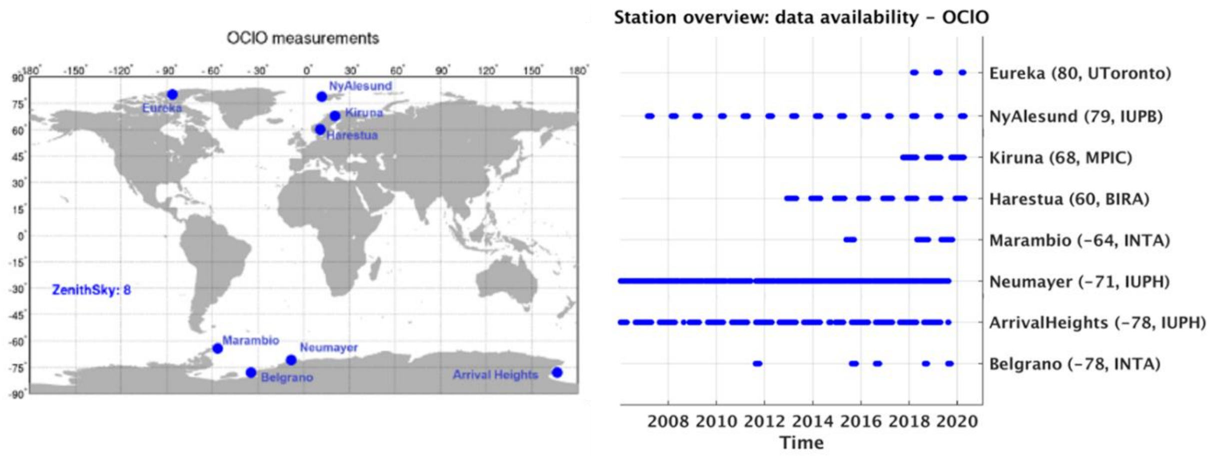

Figure 6.1: (left) Map and (right) Time-lines of ground-based OClO SCD data collected for the TROPOMI validation.

Table 6.2: Description of the different ground-based OClO datasets used in this study.

Group	Station	wavelength range (nm)	Reference spectra	Cross-sections	Other info
UToronto	Eureka	350-380	Fix, outside activation period	OClO[b] (204K), NO2[d] (220K), O3[c] (223 K), O4[f], BrO[h] (223K), Ring[i]	spectra averaged in 0.5 SZA
IUPB	NyAlesund	365-388	Fix, outside activation period	OClO[a] (213K), NO2[d] (220K, I0 corr), O4[f] (298K), Ring[j]	
MPIC	Kiruna	372 - 392	Fix, outside activation period	OClO[a] (213K), OClO$\times\lambda$, O3[c] (223K), NO2[d] (220K), O4[e] (273K), Ring (213K, 263K), $Ring_1 \times \lambda^4$, $Ring_2 \times \lambda^4$	
BIRA	Harestua	347-374	Fix, outside activation period	OClO[a] (213K), NO2[d] (220K), O3[k] (223K, 243K), BrO[g] (223K) O4[l] (293K), Ring[m]	
INTA	Belgrano, Marambio	345-389	Fix, outside activation period	OClO[a](233K), NO2[d](220K, Io corr), O4[l] (293K), Ring[i,j] (250K), BrO[h] (223K), O3[k] (223K, 243K, Io corr, with Pukite)	filter: SZA <92, RMS<1.25x10^{-3}
IUPH	Arrival Heights, Neumayer	364-391	Fix, at low SZA, outside activation period	OClO[a] (233K)	filter: SZA<94 and RMS<1x10^{-3} [Friess et al., 2005]

[a]:Kromminga et al., 2003; [b]:Wahner et al., 1987; [c]:Bogumil et al.,2003; [d]:Vandaele et al., 1997; [e]:Thalman et al., 1997; [f]:Hermans et al., 2003; [g]:Wilmouth et al., 1999; [h]:Fleischmann et al., 2004; [i]:Chance and Spurr, 1997; [j]:QDOAS high res xx; [k]:Serdyuchenko et al; [l]:Thalman and Volkamer xx ; [m]:SCIATRAN.

Limitations:

- due to the limited number of stations, spatial coverage is poor and depending on the shape of the Polar Vortex, sampling biases can occur
- ensemble of different non-harmonized analysis, with different DOAS settings (see Table 6.2)
- sensitivity to the choice of the reference spectra, that should be defined ad-hoc to not contain OClO (e.g., use a fixed yearly reference outside the activation period), otherwise it could lead to offsets in the ground-based OClO SCD.

To overcome some of these limitations, interactions with the ground-based data providers are important, and can lead to revision of some of the datasets in future versions of this report. Moreover, a post-processing of the ground-based data has also been set-up at BIRA, to try to further homogenize the data and reduce possible biases, as described in the next sub-section and used in Sect. 8.1.2.

6.1.1 Ground based OClO SCD offset correction method

For comparison with satellite measurements, total slant column measurements must be obtained. This is achieved by selecting a fixed reference spectrum taken on a clear day when the station is not under the influence of chlorine activated air masses. Usually the reference spectrum is updated each year to minimize biases due to possible instrumental instabilities. Residual offsets in the retrieved OClO SCDs may however be observed due to various possible reasons, such as (1) time-dependent instrumental effects leading to systematic spectral interference with OClO, (2) small residual OClO contamination of the selected reference spectrum, (3) spectral interference due to unknown atmospheric effects that may impact spectra and interfere with OClO retrieval.

The offset correction applied in this study is based on the assumption that the offset source (if any) is constant during a twilight period. We have build a set of solar zenith angle dependent OClO AMFs, empirically obtained from observed OClO SCDs on a few sample activated days in late February and March in Harestua. These AMFs, which include photochemical effects, are then used to build daily AM and PM OClO Langley plots, from which offset values are derived and applied to original SCDs (see Figure 6.2 for an illustration). The underlying assumption is that the OClO amount in the fixed reference spectrum is 0, and any offset found is therefore and artefact and should be removed. It must be noted that this approach is only applicable for observations covering a sufficiently large range of SZAs. The limit on the minimum solar zenith angle has been empirically set to 86 deg. For high latitude observations during polar night conditions, when the SZA constantly exceeds 86°, an estimate of the offset was obtained by fitting a polynomial function to offsets derived during the illuminated periods.

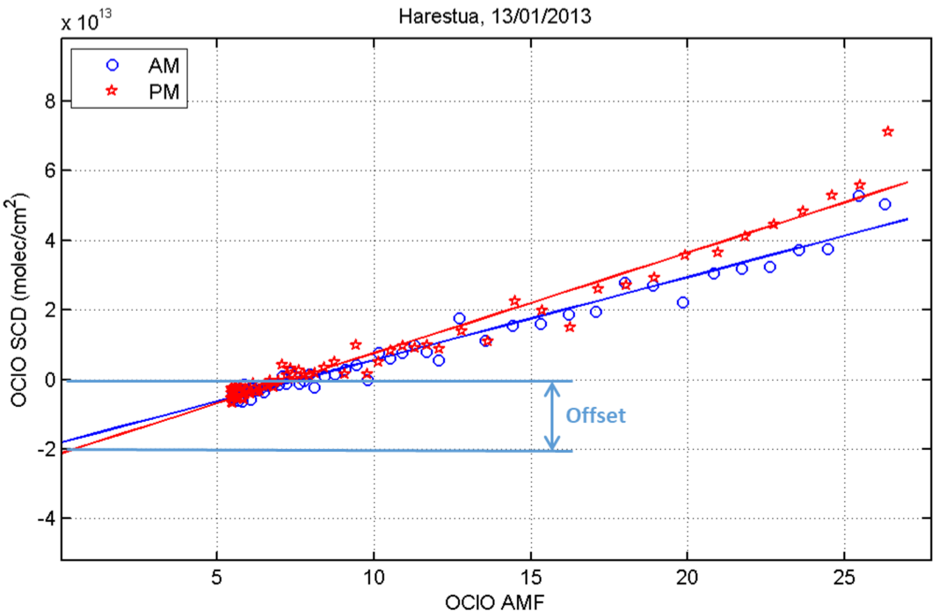

Figure 6.2: Illustration of an AM and PM OClO Langley plot for 13 January 2013 in Harestua.

This offset correction, which was derived independently for morning and evening data on each day, can be considered as objective as a) it is not linked to the satellite data and b) it is not based on subjective criteria such as the smoothness of the OClO timeseries.

7 Validation approach

The TROPOMI/S5p OClO validation approach adopted here follows the work done for the GOME-2/MetopA and -B validation within the AC SAF/EUMETSAT (Pinardi et al., 2017; Pinardi et al. in prep), and previous OClO validation studies (Richter et al., 2005; Oetjen et al., 2011). The comparison of OClO SCDs with ground-based SCD data relies on the assumption that satellite's AMF_nadir and ground-based AMF_zenith are similar. Oetjen et al. (2011) showed that AMFs from both geometries have similar values at large solar zenith angles. The AMF modelled for one day for Ny-Ålesund, based on the same model OClO vertical profile, agree within 4% in the SZA range between 89° and 91° and by 13% at 80° SZA for the two observation geometries. The sensitivity of the AMF for the two geometries will be further investigated in the future.

The TROPOMI pixels within 200km radius around each ground-based station are selected for the overpasses. A daily average of these pixels is performed, in order to improve the signal-to-noise ratio, and the values are compared to the ground-based data. Coincidences are obtained by selecting ground-based data that are within ±1° SZA of the mean daily satellite value. Error weighted averages are performed using ground-based and satellite provided errors. In a future analysis, a selection per orbit will be tested, as well as some sensitivity study on different averaging in time and space (e.g. defined by the number of pixels and number of ground based measurements).

7.1 Recommendations for data usage

For the moment, no qa_value has been defined, so all the data have been used for the validation. Several tests have been however performed, to simulate possible filter selections (limitation of the errors values, of the S5p line-of-sight by limiting the viewing zenith angle) and impacts of changing some parameters of the comparison method. These are illustrated in Sect. 8.2.

8 Status of validation

8.1 Seasonal and short term variability

This section investigates if reference measurements and TROPOMI observations are able to capture similarly the short-term variability. Illustrations are grouped by hemisphere and comparisons are performed with the original ground-based data, as received from the data providers, and then after applying the ground-based offset correction introduced in Sect. 6.1.1.

8.1.1 Original ground-based data

Data of four stations have been collected for the validation of the TROPOMI columns around Antarctica. In this region, the OClO signal is stronger in the winter months, with values up to 5-10 x10^{14} molec/cm², when the stations are within the polar vortex. The vortex is created by the large-scale descent of cold air masses during winter, with the Coriolis force leading to strong circumpolar winds that prevent inner vortex air from mixing with outer vortex air. The polar vortex is one of the most important prerequisites for the chemical destruction of stratospheric ozone in this region. While the inhomogeneous distribution of landmasses in the Northern Hemisphere leads to frequent disturbances of the Arctic vortex by vertical propagation of planetary waves, the Antarctic vortex usually is more pronounced and persistent than the Arctic one.

The daily comparisons for the Antarctic are presented in Figure 8.1, separated per year. Both 2018 and 2019 July-to-August periods show an enhanced OClO signal (from ~2 and up 5x10^{14} molec/cm²), followed by a rapid decrease, and values close to zero from October to May. Ground-based analysis for end 2019/early 2020 are not yet available, but the TROPOMI signal is similar to that of the previous years, as shown by the light magenta colors. Ground-based data from IUPH will be revisited and extended in a future version of the report, to try to investigate the negative bias in late 2018/early 2019, possibly due by a non-optimal reference spectrum choice (U. Friess personal communication).

The daily variations are sampled in a very coherent way from the ground and from space. Except for a clear negative bias in Arrival Heights (and possibly Neumayer October and November data) and a positive bias in May/June 2018 in Marambio, the satellite and ground-based data agree very well in the enhanced OClO season, and reasonably well also for low levels of OClO. The biases in this last period are possibly due to a bad choice of the reference spectrum that was not completely free of OClO or due to instrumental instabilities not accounted for. The impact of these ground-based biases is tested later on in this section with ground-based data using the offset-correction introduced in Sect. 6.1.1.

Day to day variability of several $1x10^{14}$ molec/cm² can be seen in Marambio during the activated period (June-July-August), and the saw tooth like behaviour indicates sampling of air-masses that are on the edge of the Antarctic polar vortex. The averaging of the satellite data within 200 km could mix air inside and outside the vortex, and thus a test with a selection of TROPOMI pixels within 50 km of Marambio station was done in order to try to reduce difference in vortex conditions, and presented in Figure 8.2. Small differences in the day-to-day time-series can be seen, but no big changes with respect to the baseline results of Figure 8.1.

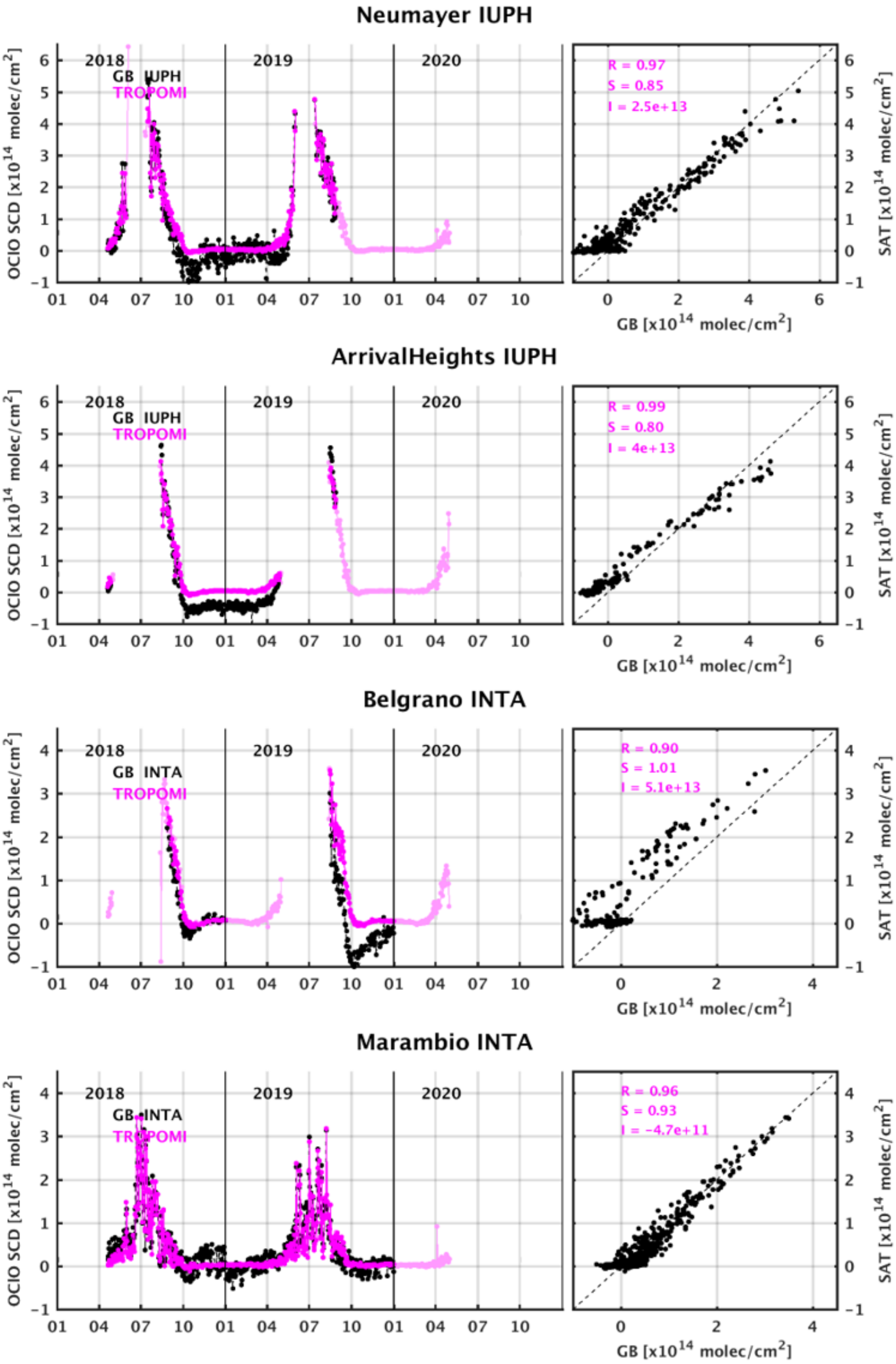

Figure 8.1: Time-series of TROPOMI and ground-based data over the Southern Hemisphere stations. Light pink are TROPOMI daily mean values, and the darker colors are the coincidences with the ground-based data. Scatter plots for each station are also included, with linear regression statistics.

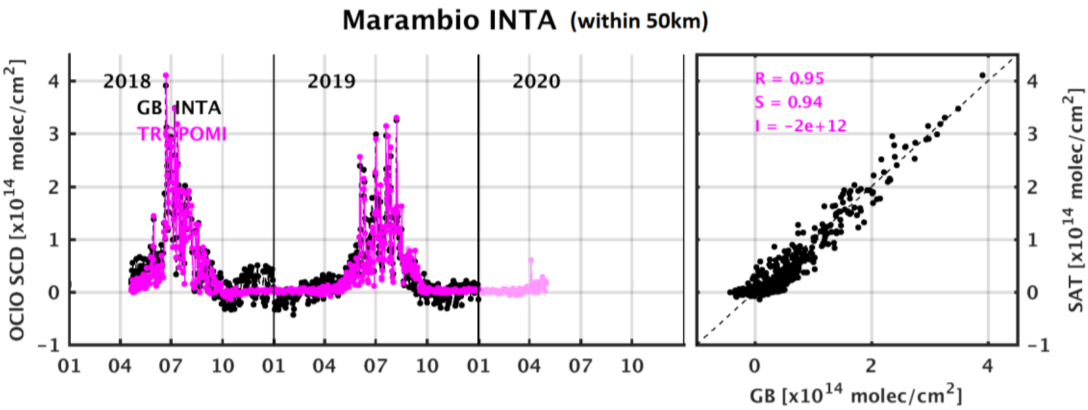

Figure 8.2: Time-series of coincident TROPOMI and Marambio ground-based data for selection of pixels within 50km around the station.

Figure 8.3 presents the daily comparisons at the four stations distributed around the Arctic Circle: Eureka on the Queen Elizabeth Islands in northern Canada, Ny-Ålesund on Spitsbergen, Kiruna in Sweden and Harestua in Norway. Data are shown for the whole year, and OClO activation periods are expected from end of winter to spring, i.e. from December to April of each year. Kiruna and Harestua have S5p data for the whole period (light magenta dots), while for Ny-Ålesund and Eureka, the day-light only starts again around February-March. The OClO signals are highest in February 2020 at the highest latitude sites, and high peaks are seen over Kiruna in winter 2019/2020. In Harestua, the OClO signal is low for all the years, with values below 5 $x10^{13}$ molec/cm², probably due to the polar vortex not extending as low as 60°N.

At all stations TROPOMI v0.9 and the zenith-sky DOAS instruments capture similarly the seasonal cycle of OClO, as well as day-to-day changes in OClO SCD. Differences from year to year and station to station exist, but typical enhanced OClO slant columns are found at the four sites in winter, with values up to $3x10^{14}$ molec/cm².

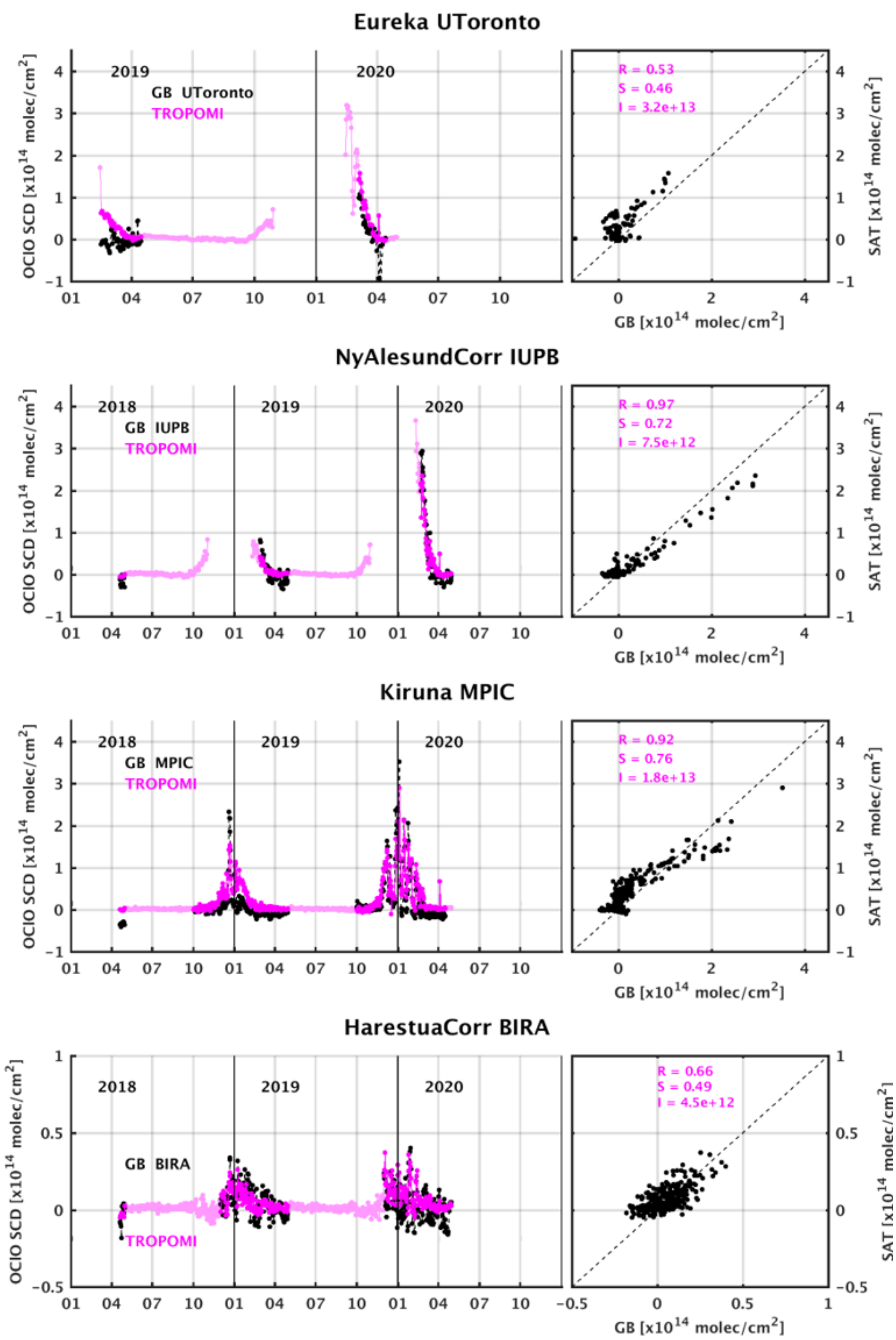

Figure 8.3: Time-series of TROPOMI and ground-based data over the Northern Hemisphere stations. Light pink are TROPOMI daily mean values, and the darker colors are the coincidences with the ground-based data. Scatter plots for each station are also included, with linear regression statistics. Note the different Y scale for Harestua.

8.1.2 Offset corrected ground-based data

As seen in Figures 8.1 and 8.3, several ground-based datasets seem to be biased in low-OClO conditions. As discussed in Section 6.1, this could be due to not-optimal selection of the reference spectra or instrumental instabilities and spectral interferences. In this section, the ground-based data were post-processed to estimate and correct for possible remaining biases, as discussed in Sect. 6.1.1. Figure 8.4 present the offset corrected comparisons for the Southern Hemisphere and Figure 8.5 for the Northern Hemisphere.

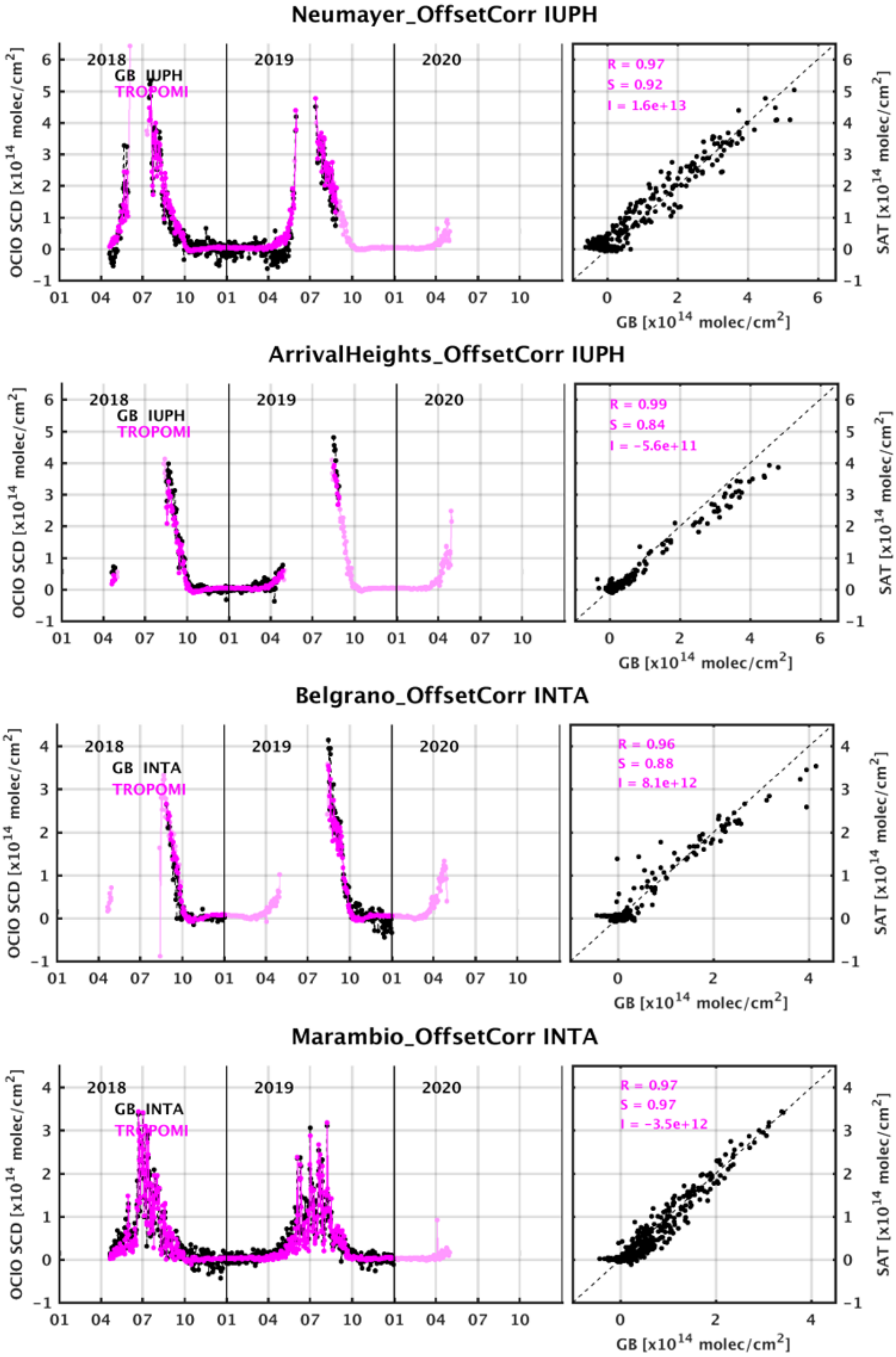

Figure 8.4: as Figure 8.1 but with the offset corrected ground-based datasets.

The clearest effect is for the stations in the Southern Hemisphere (Figure 8.4) that reported OClO SCD columns also in no-OClO periods. E.g., Arrival Heights negative data are shifted to around zero and Belgrano negative and slightly increasing data in October to December 2019 are now flattened around zero. The effect is clear when looking at the statistical parameters of the linear regression: intercepts of about 4 to 5.1 x10^{13} molec/cm² are reduced by about one order of magnitude, and changes in the slopes of about 10% are found.

Similarly, for the stations in the Northern Hemisphere, the filter is reducing the negative OClO SCD and the scatter around the zero values (e.g., Ny-Ålesund, Kiruna and Harestua) reducing the intercept of several x10^{12} molec/cm².

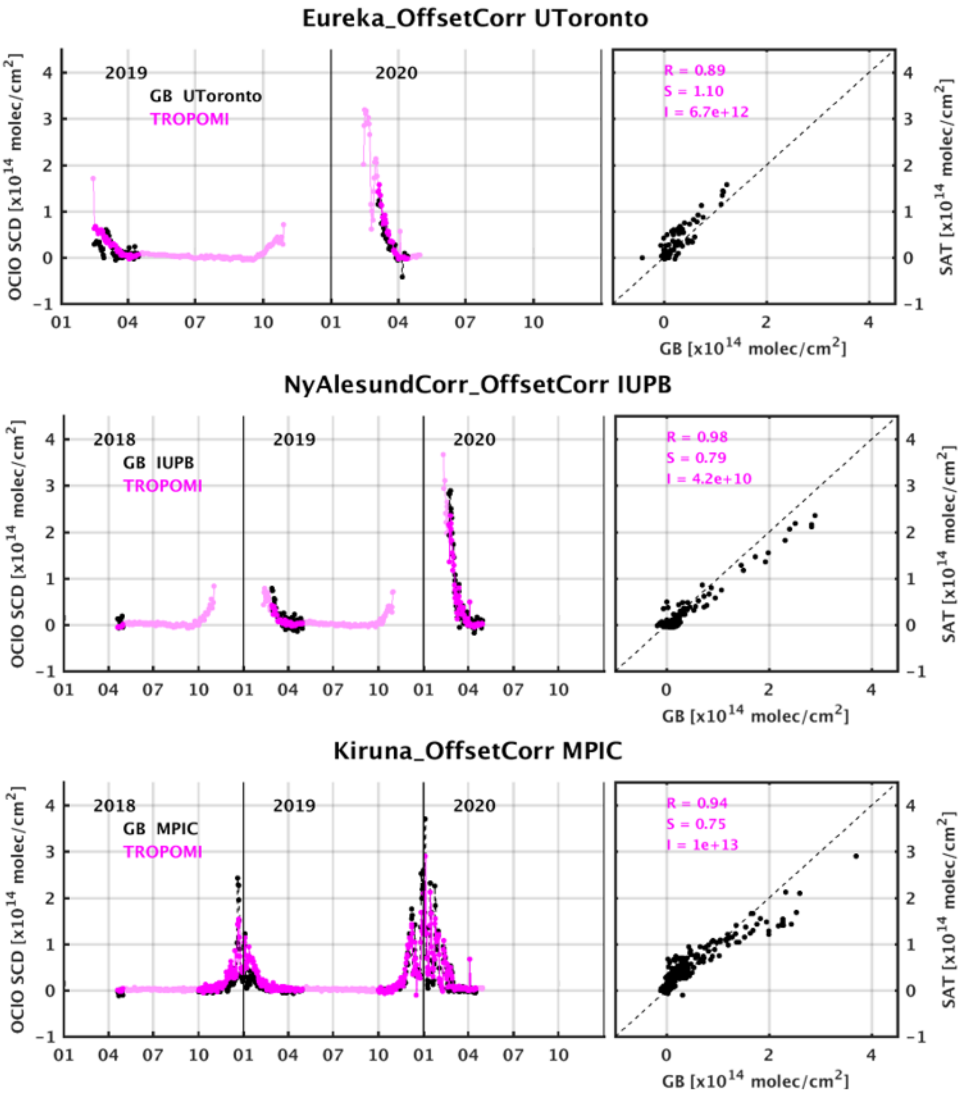

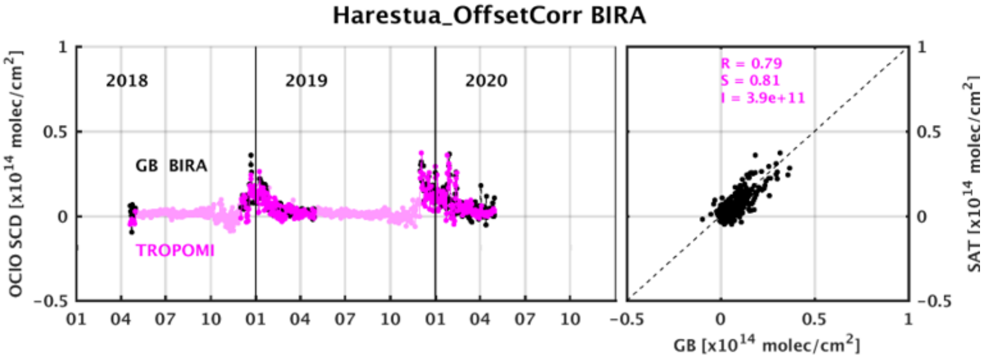

Figure 8.5: as Figure 8.3 but with the offset corrected ground-based datasets.

8.2 Scatter plots and absolute biases

The individual comparisons for Arctic and Antarctic stations after offset correction, can be synthesized in order to have a “global” view of the quality of the TROPOMI v0.9 OClO SCD product. When considering all the stations together and focusing only on the activated period (July-August-September in the Southern Hemisphere and January-February-March in the Northern Hemisphere), scatter plots of satellite versus ground-based data can be drawn, as illustrated in Figure 8.6. The correlation coefficient is about 0.97, while the regression slope is 0.9 and the intercept is less than 1 $x10^{13}$ molec/cm². If we separate these results by hemisphere, the slopes are ~ 0.88/0.82, as seen in Figure 8.7, with a larger offset in the southern Hemisphere.

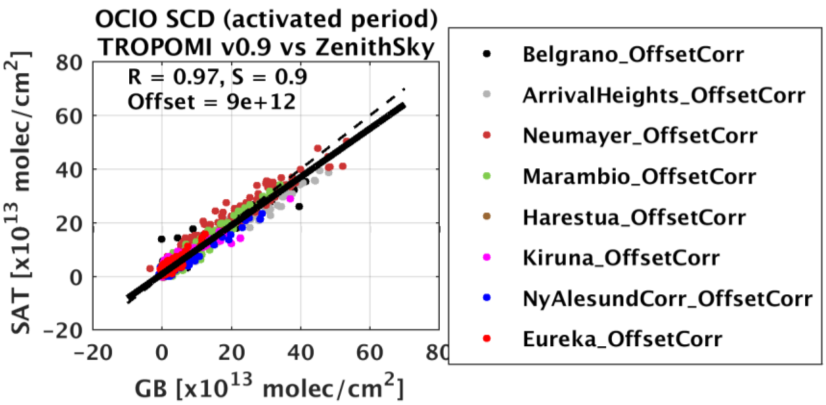

Figure 8.6: Scatter plot of TROPOMI and ground-based data over all stations, during activated months.

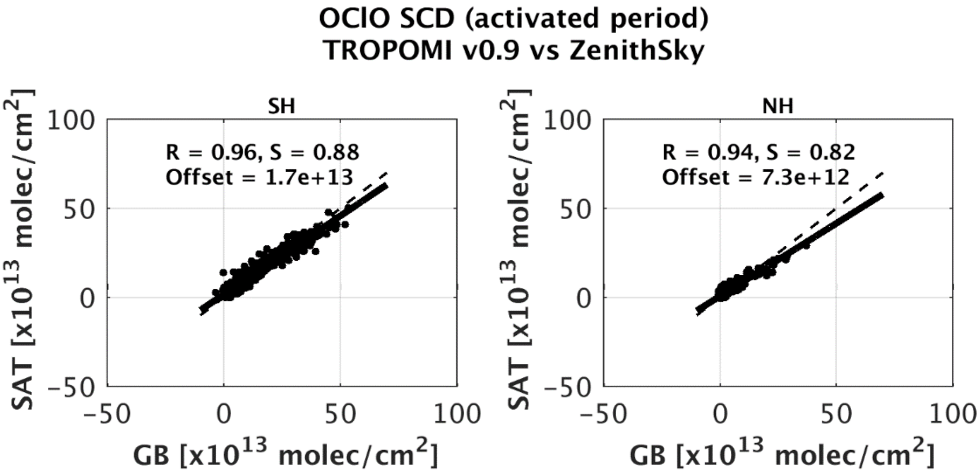

Figure 8.7: Scatter plot of TROPOMI and ground-based data over all stations, during activated months, separated per Hemisphere. Southern Hemisphere on the left panel, Northern Hemisphere on the right panel.

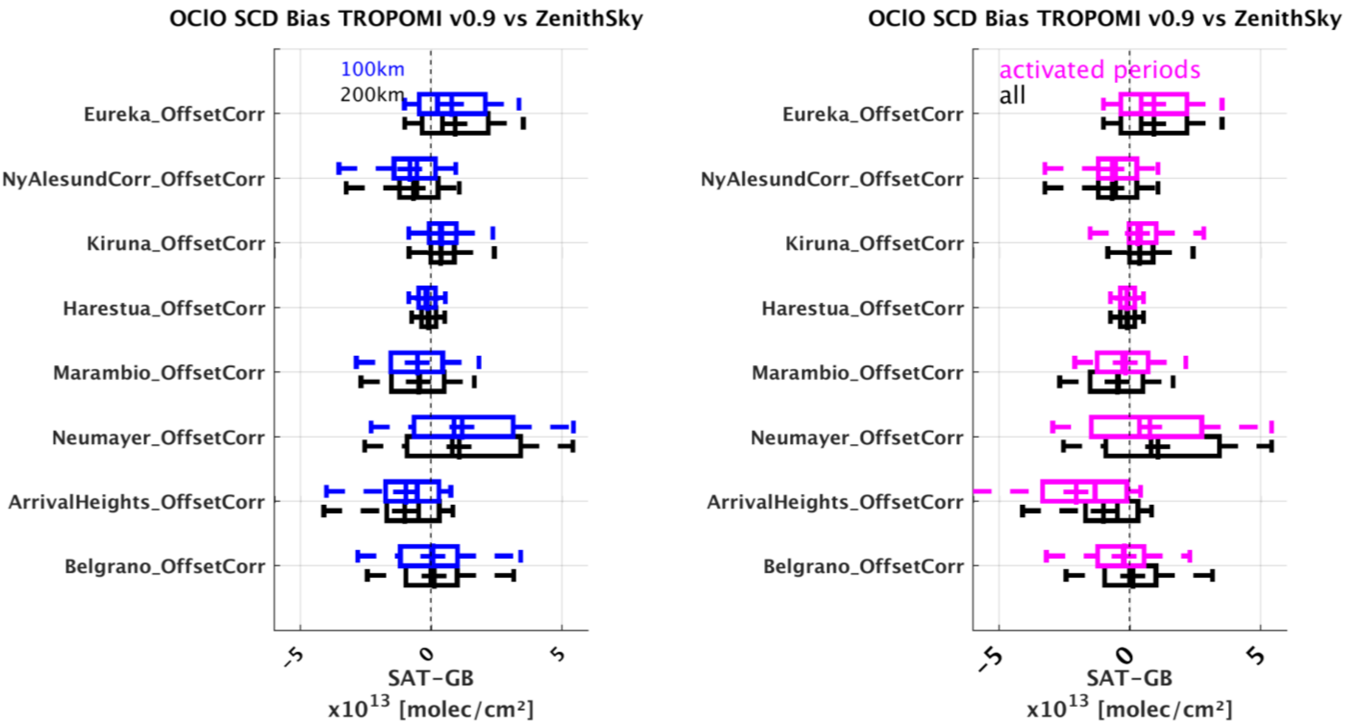

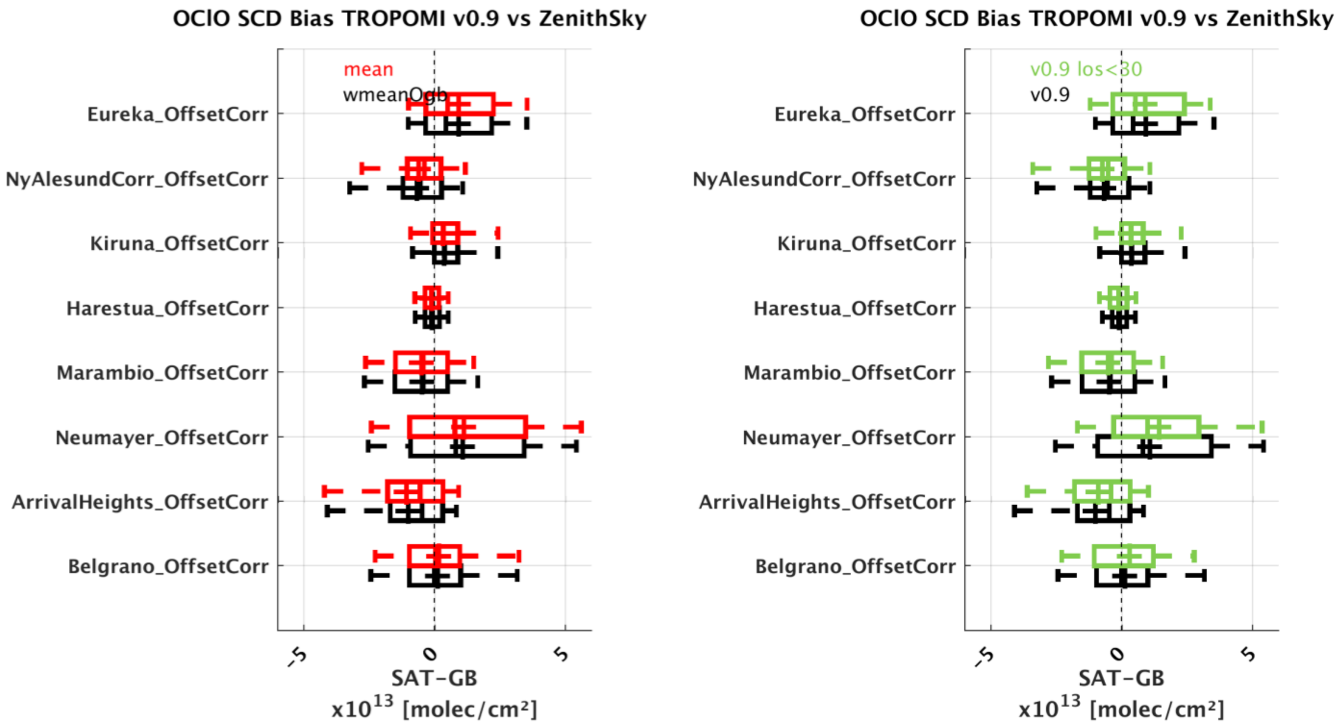

Figure 8.8: Box and whisker plot of TROPOMI minus ground-based data over all stations. Several comparison settings are compared to the baseline comparison (black). (blue) when taking a collocation radius of 100km instead of 200km; (magenta) when only considering the activated periods; (red) when doing an un-weighted average of the ground-based data ; (green) when filtering S5p for small line-of-sight (|viewing zenith angle|<30°).

The overall validation results can also be summarized with an absolute satellite minus ground-based bias estimation at each station. Figure 8.8 presents the box-and-whisker plots of these differences for each station. The box plots correspond to the 25th and 75th percentile of the distribution, while the whiskers are the 9th and 91th percentile. In addition to the results with the baseline validation approach described in Sect. 7, reported in black, additional results are reported in other colors. These tests present the results when: a) changing the colocation radius, b) only selecting activated periods, c) changing the way the daily average is done and d) limiting the S5p pixels to those having a small line-of-sight (absolute viewing zenith angle <30°). Small variability in the results is found for the different tests. The median biases at all the stations are smaller than 1 x10^{13} molec/cm² (the largest value is ~8 x10^{12} molec/cm² at Neumayer). The dispersion of the differences is generally larger than the median bias.

Figure 8.9 presents, on the left, the comparison bias and its statistical error: Err = 2*MAD/sqrt(n), where MAD is the Median Absolute Deviation (MAD = k* median(abs(bias) - median(bias)), with k = 1.4826) and n is the number of comparisons. The bias is significant if it exceeds its statistical error (presented as grey bars), which is the case in almost all the sites here. On the right of Figure 8.9, the spread of the comparison (half the interpercentile 68) is compared to the TROPOMI estimated precision of about 2.2 x10^{13} molec/cm^2 (1σ estimation from the scatter in the equatorial Pacific, [AD4]). In all cases, except Neumayer, the spread is smaller than the estimated TROPOMI precision.

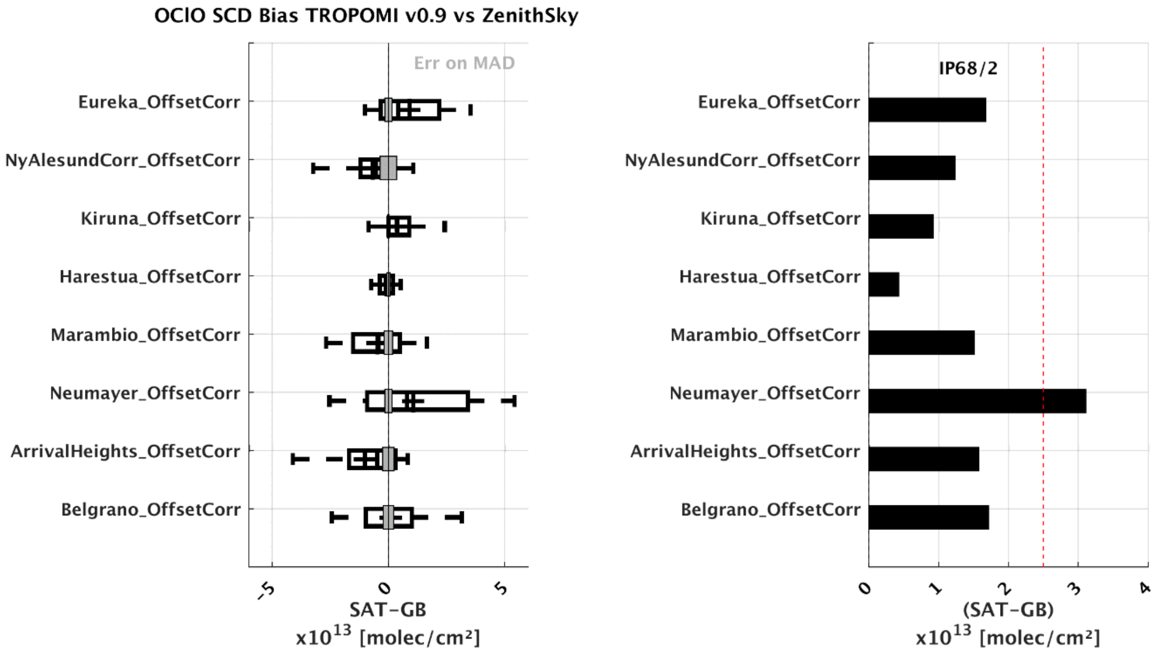

Figure 8.9: (left panel) Box and whisker plot of TROPOMI minus ground-based data and its statistical error (grey bars); (right panel) Spread on the comparison and TROPOMI estimated precision of 2.2 x10^{13} molec/cm^2.

These results indicate that the largest part of the observed offsets is linked to uncertainties in the ground-based reference data and not the TROPOMI satellite product. However, after a correction of the ground-based offsets, considering all the stations together, such as in Figure 8.7, a consistent low bias of 15 – 20% is observed in both hemispheres (overall slopes of 0.82 and 0.88).

8.3 Dependence on influencing quantities

Preliminary tests have been performed to test the dependence of the results as a function of a few influencing quantities. Figures 8.10 and 8.11 show the results for the dependence on TROPOMI SCD OClO magnitude and SZA, respectively.

It can be seen that the SAT-GB difference is larger than ±5 x10^{13} molec/cm² for SZA values above ~83° SZA, and for TROPOMI OClO SCD columns larger than 1 x10^{14} molec/cm². This behavior could be at least partly explained by the averaging of satellite data in a 200 km radius, which smears out spatially confined maxima.

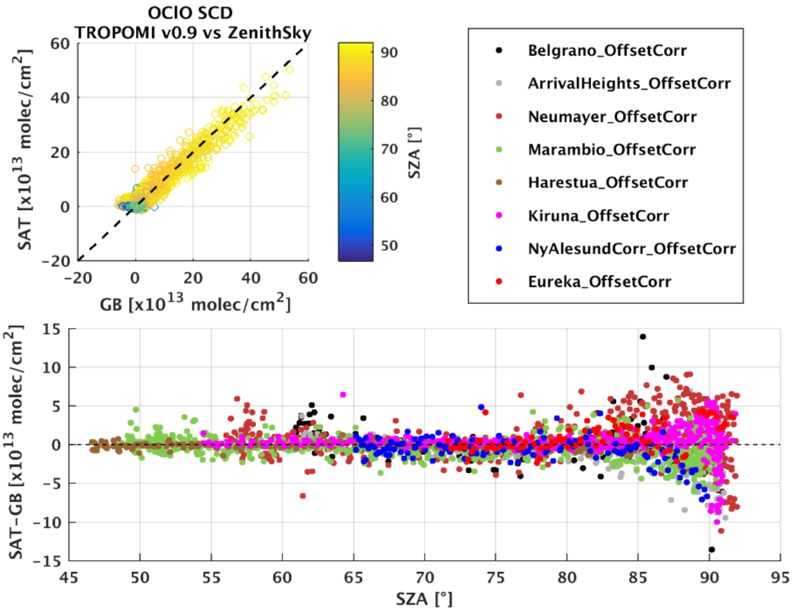

Figure 8.10: Scatter plot and absolute bias as a function of the Solar Zenith Angle, for the bias corrected ground-based sites.

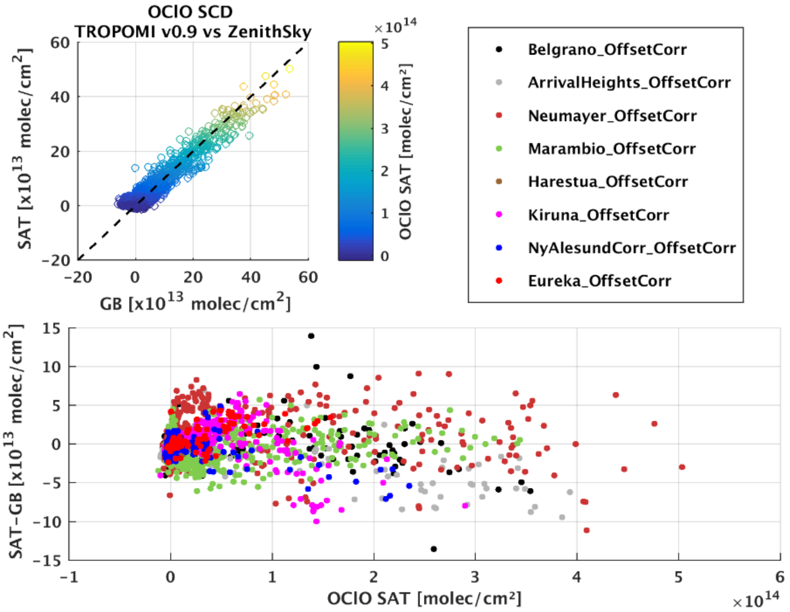

Figure 8.11: Scatter plot and absolute bias as a function of the TROPOMI OClO SCD, for the bias corrected ground-based sites.

9 Conclusions

This report investigated the quality of the S5p/TROPOMI OClO v0.9 slant columns datasets by comparing them to ground-based measurements at a selection of 8 DOAS zenith-sky stations around the Arctic and Antarctic regions: Eureka (80°N), Ny-Ålesund (79°N), Kiruna (68°N), Harestua (60°N), Marambio (64°S), Belgrano (78°S), Neumayer (71°S) and Arrival Heights (78°S). OClO spectral analyses have been performed by each data provider individually using fixed noon spectra recorded at low SZA in the absence of chlorine activation. At each station, daily comparisons are performed by selecting satellite and ground-based SCD data pairs corresponding to similar SZA conditions, and by making the assumption that the AMF is similar for satellite and ground-based measurement in these geometries.

The following main conclusions can be drawn:

- Daily mean OClO SCD time-series show that satellite and ground-based observations agree well at all stations, both in terms of seasonal and inter-annual variabilities. Variations of the OClO column, from day-to-day fluctuations to the annual cycle, are captured consistently by both measurement systems.
- Several ground-based datasets seem to be biased (e.g. negative OClO SCD during periods where we don't expect OClO). An objective offset post-correction has been set up to correct for it in a harmonized way, which improves the comparisons with S5p in term of slopes, intercept and absolute bias. Results lead to correlation coefficient of about 0.97, slope of 0.9 and intercept of less than 1 x10^{13} molec/cm². The remaining 10-20% bias could be due to the uncertainty in the zenith-sky vs nadir OClO AMF.

9.1 Improvements for next version

In the next version of the report, several aspects will be added, such as:

i. the inclusion of qa_values in the S5p OClO product, and their testing for the validation results;
ii. satellite to satellite comparisons (mainly with OMI IUPB and GOME-2 IUP datasets), also allowing more insight on the geographical patterns and probing geographical regions outside the Polar Regions;
iii. updates and improvements of the ground-based correlative datasets. This point includes the temporal extension of the datasets (such as for Arrival Heights and Neumayer stations in the Southern Hemisphere), but also a possible revision for some groups of their data, and specific analysis on the consistency of the ground-based datasets due to their different analysis settings choices (see Table 6.2), and an assessment of their consistency;
iv. sensitivity test on OClO AMF and calculation in different geometries. Ground-based zenith viewing AMF and satellite nadir viewing AMF will be calculate for an activated case, to estimate the remaining uncertainty in the SCD comparison.

10 References

Bogumil, K., Orphal, J., Homann, T., Voigt, S., Spietz, P., Fleischmann, O.C., Vogel, A., Hartmann, M., Bovensmann, H., Frerik, J., and Burrows, J. P.: Measurements of molecular absorption spectra with the SCIAMACHY Pre-Flight Model: Instrument characterization and reference spectra for atmospheric remote sensing in the 230-2380 nm region, J. Photochem. Photobiol. A, 157, 167-184, 2003.

Chance, K., and Kurucz, R. L.: An improved high-resolution solar reference spectrum for earth's atmosphere measurements in the ultraviolet, visible and near infrared, J. Quant. Spectrosc. Ra., 111, 1289-1295, 2010.

Chance, K., OMI/Aura Chlorine Dioxide (OClO) Total Column 1-orbit L2 Swath 13x24 km V003, Greenbelt, MD, USA, Goddard Earth Sciences Data and Information Services Center (GES DISC), Accessed: 14/01/2019, 10.5067/Aura/OMI/DATA2019, 2007.

Fleischmann, O. C., et al. : New ultraviolet absorption cross-sections of BrO at atmospheric temperatures measured by time-windowing Fourier transform spectroscopy, J. Photochem. Photobiol. A, 168, 117–132, 2004.

Friess, U., Kreher, K., Johnston, P. V., and Platt, U.: Ground-based DOAS measurements of stratospheric trace gases at two Antarctic stations during the 2002 ozone hole period, J. Atmos. Sci., 62, 765–777, 2005.

Gil, M., Puentedura, O., Yela, M., Parrondo, C., Jadhav, D. B., and Thorkelsson, B.: OClO, NO2 and O3 total column observations over Iceland during the winter 1993/94, *Geophys. Res. Lett.*, **23**, 3337–3340, 1996.

Hendrick, F., Van Roozendael, M., Kylling, A., Petritoli, A., Rozanov, A., Sanghavi, S., Schofield, R., von Friedeburg, C., Wagner, T., Wittrock, F., Fonteyn, D. and De Mazière, M.: Intercomparison exercise between different radiative transfer models used for the interpretation of ground-based zenith-sky and multi-axis DOAS observations, Atmos. Chem. Phys., 6, 93–108, doi:10.5194/acp-6-93-2006, 2006.

Hermans, C., Vandaele, A. C., Carleer, M., Fally, S., Colin, R., Jenouvrier, A., Coquart, B., and Merienne, M.-F.: Absorption cross-sections of atmospheric constituents: NO2, O2, and H2O, Environ. Sci. Pollut. R., 6, 151–158, 1999.

Kreher, K., Keys, J. G., Johnston, P. V., Platt, U., and Liu, X.: Ground-based measurements of OClO and HCl in austral spring 1993 at Arrival Heights, Antarctica, *Geophys. Res. Lett.*, **23**, 1545–1548, 1996.

Kromminga, H., Orphal, J., Spietz, P., Voigt, S., and Burrows, J. P.: New measurements of OClO absorption cross-sections in the 325-435 nm region and their temperature dependence between 213 and 293 K, J. Photoch. Photobio. A, 157, 149–160, 2003.

Oetjen, H., Wittrock, F., Richter, A., Chipperfield, M. P., Medeke, T., Sheode, N., Sinnhuber, B.-M., Sinnhuber, M., and Burrows, J. P.: Evaluation of stratospheric chlorine chemistry for the Arctic spring 2005 using modelled and measured OClO column densities, *Atmos. Chem. Phys.*, **11**, 689-703, doi:10.5194/acp-11-689-2011, 2011.

Pinardi, G., Van Roozendael, M., Hendrick, F., Valks, P., : Validation report of GOME-2 GDP 4.8 OClO slant column data record for MetOp-A and -B DRR , AC SAF validation report, SAF/AC/IASB/VR/OClO, 29 May 2017 (https://acsaf.org/docs/vr /Validation_Report_DR_OClO_GDP48_May_2017.pdf

Pinardi, G., Van Roozendael, M., Hendrick, Richter, A., Valks, P., Bognar, K., Frieß, U., Granville, J., Gu, M., Johnston, P., Prados-Roman, C., Puentedura, O., Querel, R., Strong, K., Wagner, T., Wittrock, F. and Yela Gonzalez, Y. : Ground-based validation of the MetopA and B GOME-2 OClO measurements, in preparation for AMT.

Puentedura, O., Yela, M., Navarro-Comas, M., Igleias, J., Ochoa, H., Halogen oxides from MAXDOAS observations at Belgrano II station (Antarctica, 78°S) in 2013, EGU poster 2014.

Richter A., Slijkhuis S., Loyola D., Offline Total OClO validation report, O3M-11, 2009. (http://www.iup.uni-bremen.de/doas/reports/o3saf_vs_gome-2_oclo_finalreport_091208.pdf)

Richter, A., F. Wittrock, M. Weber, S. Beirle, S. Kühl, U. Platt, T. Wagner, W. Wilms-Grabe, and J. P. Burrows, GOME observations of stratospheric trace gas distributions during the splitting vortex event in the Antarctic winter 2002 Part I: Measurements, J. Atmos. Sci., 62 (3), 778-785, 2005.

Richter, A., M. Eisinger, A. Ladstätter-Weißenmayer and J. P. Burrows, DOAS zenith sky observations. 2. Seasonal variation of BrO over Bremen (53°N) 1994-1995, *J. Atm. Chem.*, **32**, 83-99, 1999.

Richter, A.: Absorptionsspektroskopische Messungen stratosphärischer Spurengase über Bremen, 53° N, PhD thesis, University of Bremen. Available from: http://www.iup.uni-bremen.de/doas/paper/diss_97_richter.zip, 1997.

Richter. A., Wittrock, F:, Valks, P., Evaluation of the possibility to derive reliable OClO slant columns from GOME2b and GOME2a spectra, O3M SAF VSA ID O3_AS14_02 final report, 2015 (http://www.iup.uni-bremen.de/doas/reports/o3m-saf_oclo_2_report_160427.pdf).

Rigby, M., Park, S., Saito, T., Western, L. M., Redington, A. L., Fang, X., Henne, S., Manning, A. J., Prinn, R. G., Dutton, G. S., Fraser, P. J., Ganesan, A. L., Hall, B. D., Harth, C. M., Kim, J., Kim, K. R., Krummel, P. B., Lee, T., Li, S., Liang, Q., Lunt, M. F., Montzka, S. A., Mühle, J., O'Doherty, S., Park, M. K., Reimann, S., Salameh, P. K., Simmonds, P., Tunnicliffe, R. L., Weiss, R. F., Yokouchi, Y. and Young, D.: Increase in CFC-11 emissions from eastern China based on atmospheric observations, Nature, 569(7757), 546–550, doi:10.1038/s41586-019-1193-4, 2019.

Rozanov, V. V., Rozanov, A. V., Kokhanovsky, A. A. and Burrows, J. P.: Radiative transfer through terrestrial atmosphere and ocean: Software package SCIATRAN, J. Quant. Spectrosc. Radiat. Transf., 133, 13–71, doi:10.1016/j.jqsrt.2013.07.004, 2014.

Serdyuchenko, A., Gorshelev, V., Weber, M., Chehade, W. and Burrows, J. P.: High spectral resolution ozone absorption cross-sections – Part 2: Temperature dependence, Atmos. Meas. Tech., 7(2), 625–636, doi:10.5194/amt-7-625-2014, 2014.

Sinnhuber, B. M., Weber, M., Amankwah, A. and Burrows, J. P.: Total ozone during the unusual Antarctic winter of 2002, Geophys. Res. Lett., 30(11), 10–13, doi:10.1029/2002GL016798, 2003.

Solomon, S., Mount, G. H., Sanders, R. W., and Schmeltekopf, A. L.: Visible Spectroscopy at McMurdo Station, Antarctica – 2. Observations of OClO, J. Geophys. Res., 92, 8329–8338, 1987.

Solomon, S., Mount, G. H., Sanders, R. W., Jakoubek, R. O., and Schmeltekopf, A. L.: Observations of the nighttime abundance of OClO in the winter stratosphere above Thule, Greenland, *Science*, **242**, 550–555, 1988.

Tørnkvist, K. K., Arlander, D. W., and Sinnhuber, B. M.: Ground-based UV measurements of BrO and OClO over Ny-Ålesund during winter 1996 and 1997 and Andøya during winter 1998/1999, *J. Atmos. Chem.*, **43**, 75–106, 2002.

Valks, P., Loyola, D., Hao, N., Hedelt, P., Slijkhuis, S., Grossi, M., Gimeno Garcia, S., Lutz, R., ATBD GOME-2 Total Column Products of Ozone, NO2, BrO, HCHO, SO2, H2O, OClO and Cloud Properties, https://acsaf.org/docs/atbd/Algorithm_Theoretical_Basis_Document_NTO_OTO_DR_GDP48_Jun_2017.pdf, 2017

Vandaele, A. C., Hermans, C., Fally, S., Carleer, M., Colin, R., Mérienne, M. F., Jenouvrier, A. and Coquart, B.: High-resolution Fourier transform measurement of the NO2 visible and near-infrared absorption cross sections: Temperature and pressure effects, J. Geophys. Res. Atmos., 107(18), doi:10.1029/2001JD000971, 2002.

Wagner, T., Leue, C., Pfeilsticker, K. and Platt, U.: Monitoring of the stratospheric chlorine activation by Global Ozone Monitoring Experiment (GOME) OClO measurements in the austral and boreal winters 1995 through 1999, J. Geophys. Res. Atmos., 106(D5), 4971–4986, doi:10.1029/2000JD900458, 2001.

Wagner, T., Wittrock, F., Richter, A., Wenig, M., Burrows, J. P., and Platt, U.: Continuous monitoring of the high and persistent chlorine activation during the Arctic winter 1999/2000 by the GOME instrument on ERS-2, J. Geophys. Res.-Atmos., 107, 8267, doi:10.1029/2001JD000466, 2002.

Wahner, A., G. S. Tyndall, and A. R. Ravishankara (1987), Absorption Cross-Sections for Ocio as a Function of Temperature in the Wavelength Range 240-480 Nm, J Phys Chem-Us, 91(11), 2734-2738.

Wittrock, F., Oetjen, H., Richter, A., Fietkau, S., Medeke, T., Rozanov, A., and Burrows, J.P. (2004), MAX-DOAS measurements of atmospheric trace gases in Ny-Ålesund – Radiative transfer studies and their application, Atmos. Chem. Phys., 4, 955–966, doi:10.5194/acp-4-955-2004.

Yela, M., C. Parrondo, M. Gil, S. Rodríguez, J. Araujo, H. Ochoa, G. Deferrari and S. Díaz, The September 2002 Antarctic vortex major warming as observed by visible spectroscopy and ozonesoundings. International Journal of Remote Sensing, V26, N16, 3361-3376, 2005.